European blocking and Atlantic jet stream variability in the NCEP/NCAR reanalysis and the CMCC-CMS climate model

**Paolo Davini · Chiara Cagnazzo · Pier Giuseppe Fogli ·
Elisa Manzini · Silvio Gualdi · Antonio Navarra**

Abstract The relationship between atmospheric blocking over Europe and the Atlantic eddy-driven jet stream is investigated in the NCEP/NCAR Reanalysis and in a climate model. This is carried out using a bidimensional blocking index based on geopotential height and a diagnostic providing daily latitudinal position and strength of the jet stream. It is shown that European Blocking (EB) is not decoupled from the jet stream but it is mainly associated with its poleward displacements. Moreover, the whole blocking area placed on the equatorward side of the jet stream, broadly ranging from Azores up to Scandinavia, emerges as associated with poleward jet displacements. The diagnostics are hence applied to two different climate model simulations in order to evaluate the biases in the jet stream and in the blocking representation. This analysis highlights large underestimation of EB, typical feature of general circulation models. Interestingly, observed blocking and jet biases over the Euro-Atlantic area are consistent with the blocking-jet relationship observed in the NCEP/NCAR Reanalysis. Finally, the importance of sea surface temperatures (SSTs) is investigated showing that realistic SSTs can reduce the bias in the jet stream variability but not in the frequency of EB. We conclude highlighting that blocking-related diagnostics can provide more information about the Euro-Atlantic variability than diagnostics simply based on the Atlantic jet stream.

Keywords Atlantic jet stream · European blocking · Climate model · SSTs

P. Davini (✉) · P. G. Fogli · S. Gualdi · A. Navarra
Centro Euro-Mediterraneo sui Cambiamenti Climatici (CMCC), Bologna, Italy
e-mail: p.davini@isac.cnr.it

P. Davini
Ca' Foscari University, Venezia, Italy

Present Address:
P. Davini
Istituto di Scienze dell'Atmosfera e del Clima (ISAC-CNR), Corso Fiume 4, Torino 10133, Italy

C. Cagnazzo
ISAC-CNR, Roma, Italy

E. Manzini
Max Plank Institute for Meteorology, Hamburg, Germany

S. Gualdi · A. Navarra
Istituto Nazionale di Geofisica e Vulcanologia, Bologna, Italy

1 Introduction

The Euro-Atlantic region shows a great amount of natural variability, with weather phenomena acting on different spatial and temporal scales, ranging from synoptic scale cyclones up to large-scale planetary wave oscillations. Further interest in the last years has been raising around the role of low-frequency anomalies associated with atmospheric blocking, a mid-latitude weather pattern that describes a quasi-stationary, long-lasting, high-pressure system that modifies the westerly flow, "blocking" (or at least diverting) the eastward movement of the migratory cyclones (Rex 1950). Blocking has also been associated with the concept of Rossby Wave Breaking (RWB, Pelly and Hoskins 2003; Tyrlis and Hoskins 2008), a large-scale reversal of the potential vorticity gradient on an isentropic surface (McIntyre and Palmer 1983). RWB can be categorized into cyclonic and anticyclonic events according to the tilt and the direction of rotation of the trough-ridge pair (Thorncroft et al. 1993; Peters and Waugh 1996).

Atmospheric blocking can be detected with different objective methods (Dole and Gordon 1983; Tibaldi and Molteni 1990; Pelly and Hoskins 2003; Barriopedro et al. 2010; Barnes et al. 2011). Recently Davini et al. (2012, D12 herafter) performed a detailed phenomenological analysis of Northern Hemisphere blocking, accounting for several diagnostics including the orientation of the RWB associated with the blocking events. Making use of a bidimensional index based on geopotential height, they showed that it is possible to distinguish among three main categories of blocking. The first one, placed at high latitudes, is defined as High Latitude Blocking (Berrisford et al. 2007; Woollings et al. 2008), and it collects the bulk of the events over the Eastern Siberia/North Pacific (North Pacific Blocking) and over Greenland (Greenland Blocking, GB). These blocking events are characterized by long duration (on the order of 9 days), by a cyclonic RWB events associated with them and by an East/West tilt. Making use of two different intensity diagnostics, D12 confirmed that these events are not able to block the flow but they only divert it southward.

A second category of blocking includes an anomalous group of events that is not commonly identified as blocking. Indeed, they are detected approximatively south of 40° N, over the Eastern Pacific and the Eastern Atlantic oceans. Due to their peculiar position, these events have been defined as Low Latitude Blocking (LLB); they are unable to divert or block the flow and they are just a manifestation of the oscillation of the subtropical high pressure system. They are characterized by an anticyclonic RWB of the Atlantic Ridge, average duration of about 7 days and by an equivalent barotropic structure.

Finally, the third category of blocking includes events placed at mid-latitude that are actually able to block the westerly flow. D12 pointed out a marked difference in mid-latitude blocking activity over the Pacific and the Atlantic ocean, showing that these events are evident at the exit of Atlantic jet stream only, over the European continent. Therefore these blocking events are defined as European Blocking (EB). EB presents similar characteristics with respect to LLB (equivalent barotropic cross section, similar duration and anticyclonic orientation of wave breaking), even though they are placed farther Northeast and they have a large impact on the European weather.

In the literature, a topic of well-known interest is the one that tries to reconcile these different categories of atmospheric blocking with the other main elements of variability of the mid-latitude climate. Indeed, several authors have investigated the connection between blocking, Rossby Wave Breaking, the main teleconnection patterns and the jet stream variability.

For instance, many works found evidence of a relationship between the North Atlantic Oscillation (NAO, the dipole of the high and low pressure between Azores and Iceland, Hurrel et al. 2003) and Rossby Wave Breaking (Benedict et al. 2004; Franzke et al. 2004; Riviere and Orlanski 2007; Kunz et al. 2009a, b).

A group of recent papers (Croci-Maspoli et al. 2007; Woollings et al. 2008, 2010a) showed that the phase of the NAO is strongly linked with the presence or absence of blocking over Greenland. This interpretation of the NAO as a dualism between a "blocked" and a "non-blocked" state fits notably well with observational data (Woollings et al. 2008). The negative phase of the NAO is largely correlated with the presence of blocking over Greenland (GB), and with an associated southward shift of the eddy driven jet stream, which merges with the subtropical jet (Woollings et al. 2010b; Athanasiadis et al. 2010).

Other works analyzed the latitudinal position and the persistence of the Atlantic eddy-driven jet stream (Barnes and Hartmann 2010; Barnes et al. 2010; Kidston and Vallis 2010) and the association between the jet shifts and the NAO (Strong and Davis 2008; Athanasiadis et al. 2010). Much of the wintertime Euro-Atlantic variability can be associated with the low-level westerly winds blowing over the Atlantic ocean. Woollings et al. (2010a) analyzed the displacements of the Atlantic jet stream in association with the occurrence of Rossby Wave Breaking (and consequently, with blocking). They found a trimodal distribution of the latitudinal position of the eddy jet stream, detecting a central "non-perturbed" state of the jet and two different equatorward and poleward preferential positions. They showed that the NAO is unable to fully describe the Atlantic jet variability, which can be only explained by a combination of the first two Atlantic Empirical Orthogonal Functions (EOFs). They also highlighted that while the equatorward shift seems to be tightly coupled to the occurrence of GB events, it is harder to find a blocking region clearly linked to the northward jet displacements. Indeed, they suggested that EB is decoupled from the Atlantic jet stream.

However, as mentioned before, D12 highlighted the strong impact on the zonal and meridional flow played by the EB. Therefore, starting from the work performed by Woollings et al (2010a) and exploiting the climatology developed by D12, the purpose of our work is to address the relationship between atmospheric blocking and Atlantic jet stream displacements, investigating the possibility that EB is not decoupled from the jet variability. This relationship will be investigated using daily data from the NCEP/NCAR Reanalysis (Kalnay et al. 1996), adopting a bidimensional blocking index based on the geopotential height and a measure of the daily jet speed and latitude.

Furthermore, it is well known that state of the art climate models exhibit large bias in the representation of EB (D'Andrea et al. 1997; Scaife et al. 2010). Therefore, we

will apply blocking and jet diagnostics to an atmosphere-only and fully-coupled runs of the CMCC-CMS climate model, in order to evaluate their biases and understand what diagnostics provide more information about the Euro-Atlantic variability. In this context, we will investigate the blocking-jet stream relationship and the role of the sea surface temperatures (SSTs) in modulating these phenomena.

2 Data and method

The data adopted in this study is the daily NCEP/NCAR Reanalysis (Kalnay et al. 1996), from which the 55-year period from 1951 to 2005 was selected. The period analyzed includes the winter season (DJF) for a total number of 4,964 days. Only events occurring in the Northern Hemisphere are analyzed. All data have the standard NCEP/NCAR resolution of 2.5° × 2.5°.

The Centro Euro-Mediterraneo sui Cambiamenti Climatici Climate Model with a resolved Stratosphere (CMCC-CMS) is based on the MA-ECHAM5 (Middle Atmosphere ECHAM5) atmospheric component (Roeckner et al. 2006; Manzini et al. 2006), the OASIS3 coupler (Valcke 2006; Fogli et al. 2009) and the OPA8.2/LIM ocean and sea-ice components (Madec et al. 1998; Fichefet and Morales-Maqueda 1997). The oceanic component has a constant resolution of about 2 degrees in horizontal and 31 vertical levels. The atmospheric configuration adopted here (T63L95) has a high vertical resolution (95 levels), a high top (up to 80 km) and a horizontal resolution of about 1.8 × 1.8 deg (Manzini et al. 2012). This version of MA-ECHAM5 includes the parameterization of momentum conserving orographic and non-orographic gravity wave drag. The shortwave radiation scheme covers the 185–4,000 nm spectral interval with a spectral resolution of 6 bands separating the UV and visible ozone absorption (Cagnazzo et al. 2007).

In this work we make use of data from two different experiments, both performed for the Coupled Model Intercomparison Project Phase 5 (CMIP5). The first one, hereafter called HIST, is a historical fully-coupled numerical experiment (DJF 1951–2005) of the CMCC-CMS climate model. The second one, hereafter named AMIP, is the corresponding atmosphere-only run (DJF 1951–2005) of the CMCC-CMS with prescribed SST. The imposed SST are the HadISST (Rayner et al. 2003). For both simulations, the forcing data are specified following the CMIP5 protocol. Specifically, well-mixed greenhouse gases are specified individually to the radiation code as CO_2, CH_4, N_2O, CFC-11, CFC-12 and HFC-134-equivalent; anthropogenic three-dimensional sulphate aerosol concentrations are specified considering the direct and first

indirect effect; the total solar irradiance (TSI) and the percentage of irradiance in each of the shortwave model radiation bands vary with an 11-year solar cycle (for the TSI an anomaly is added to the 1,367 Wm^{-2}); specified monthly-mean ozone fields include variations associated to the solar cycle. Different from the CMIP5 recommendations, the historical ozone is extended to the top of the model (0.01 hPa, whereas the CMIP5 data stopped at 10 hPa).

The model outputs are interpolated on the 2.5° × 2.5° grid in order to facilitate the comparison with NCEP/NCAR Reanalysis. As a consequence of a storage failure, December 1957 for the HIST run is not available.

In order to objectively detect atmospheric blocking a bidimensional index based on the reversal of the meridional gradient of geopotential height at 500 hPa is adopted (Tibaldi and Molteni 1990; Scherrer et al. 2006; D12). For every grid point of coordinates (λ_0, Φ_0) we define:

$$GHGS(\lambda_0, \Phi_0) = \frac{Z500(\lambda_0, \Phi_0) - Z500(\lambda_0, \Phi_S)}{\Phi_0 - \Phi_S}, \quad (1)$$

$$GHGN(\lambda_0, \Phi_0) = \frac{Z500(\lambda_0, \Phi_N) - Z500(\lambda_0, \Phi_0)}{\Phi_N - \Phi_0} \quad (2)$$

where Φ_0 ranges from 30° to 75°N and λ_0 ranges from 0° to 360°. $\Phi_S = \Phi_0 - 15°, \Phi_N = \Phi_0 + 15°$. Therefore an Instantaneous Blocking (IB) is identified if:

$$GHGS(\lambda_0, \Phi_0) > 0 \quad GHGN(\lambda_0, \Phi_0) < -10 \text{ m}/°lat \quad (3)$$

In order to ensure that spatial and temporal scales are significant to detect a blocking event, some constraints have been applied to the Instantaneous Blocking previously defined: an IB must be extended for at least 15° of continuous longitude. Finally, a Blocking Event is defined when blocking is occurring within a box of 10° longitude × 5° latitude around that point for at least 5 days. This method allows the computation of single event duration as well as the average values of duration of the Blocking Events for each grid point. Furthermore, two different intensity index and a measure of the direction of the rotation of the Rossby Wave Breaking associated with the blocking have been used. Full details on the blocking detection scheme and the related diagnostics can be found in D12.

To study the daily changes of the position of the eddy-driven jet stream, we introduce the Jet Latitude Index (JLI) following Woollings et al. (2010a). The JLI expresses the latitude of the zonally averaged maximum of the zonal wind speed between 60° and 0° W longitude. The wind zonal speed is vertically averaged from 925 to 700 hPa. The daily values of the JLI express a measure of the latitudinal position of the Atlantic eddy-driven jet, each day. For our work a slightly different version of this index is

adopted, based on 5-day running-mean data and on absolute latitude values. In addition to the daily latitudinal position, we will make use of the daily value of zonally averaged maximum of zonal wind speed in order to provide information on the jet strength.

3 Results

3.1 Blocking and Atlantic jet stream climatology

Figure 1 (left) shows the DJF blocking climatology over the Euro-Atlantic region for the 1951–2005 NCEP/NCAR Reanalysis expressed as the percentage of blocked days per season. At high latitudes, a relative maximum is visible over Greenland (GB). It is possible to observe also a large maximum located over North-Western Europe, between Norway and Great Britain, which identifies the EB events. A band of high values associated with this maximum develops almost uniformly to the subtropics over Central Eastern Atlantic, where a further relative maximum is observed. These latter events have been defined as LLB and they have been widely investigated by D12.

The right panel of Fig. 1 shows the climatology for the same period for the Atlantic eddy-driven jet stream. It is reported as a bidimensional PDF showing the JLI on the x-axis and the jet speed on the y-axis. With respect to the 1-dimensional JLI PDF reported in Fig. 1 of Woollings et al. (2010a) some minor differences can be seen in the proportion of the peaks, with the southern one not clearly evident. However, the trimodal nature of the Atlantic JLI PDF is preserved (see also Fig. 6). The most interesting

result emerging from Fig. 1 is the higher values of jet speed for the central peak, about 2–3 m/s larger than for the poleward and equatorward peak.

3.2 The relationships between blocking and the Atlantic jet stream

In order to analyze the relationship between the Atlantic jet stream and the blocking events, we focused our analysis on four lat-lon sectors, whose coordinates are reported in Table 1 and whose areas are shown in the left panel of Fig. 1. Those sectors have been defined as boxes centered on the relative maximum of Blocking Events frequency in the considered area. In addition to the already mentioned GB, EB and Atlantic LLB, a further sector defined as Iberian Wave Breaking (IWB) is introduced. This sector, over Eastern Atlantic off the coast of Western Europe, is similar to the one defined in previous works (Woollings et al. 2010a, 2011) and it covers the blocking area on the equatorward side of the jet that is not included in the EB and LLB sectors.

Using daily data, a sector is considered as blocked when at least one blocked grid point is detected within the box. Therefore it is possible to create a daily binary timeseries (that provides the blocked or non-blocked state of the sector) for each sector.

Composites on blocked days for the position and strength of the Atlantic jet-stream are computed for each sector and they are shown in Fig. 2. The upper left panel shows the well-established relationship linking the occurrence of Greenland Blocking with southward displacement of the jet stream (Woollings et al. 2010a). A clear
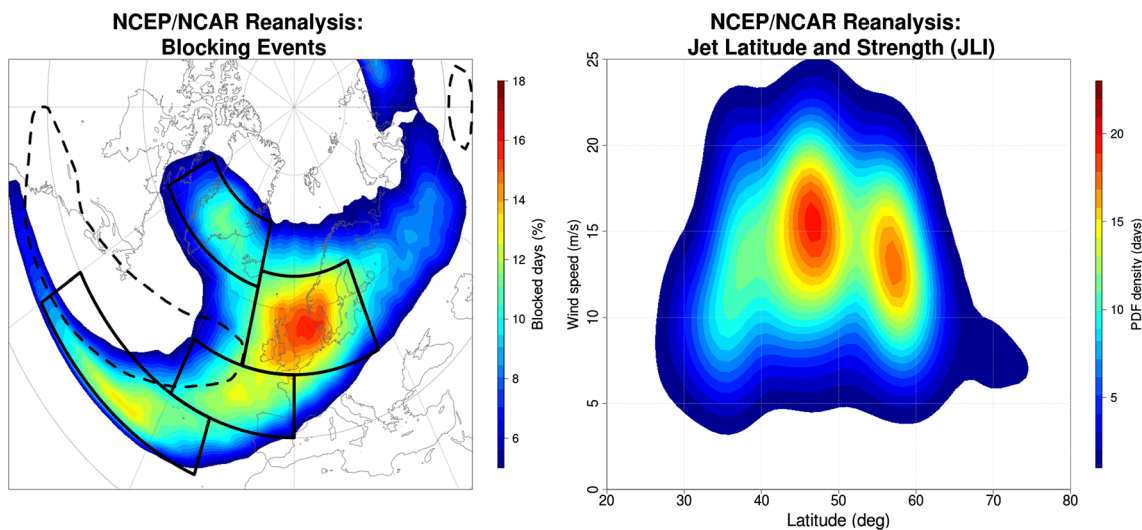

Fig. 1 *Left panel*: blocking events frequency. *Colours* are representative of percentage of blocked days per season. *Dashed black contours* show the eddy driven jets as climatological zonal wind speed higher than 8 m/s at 850 hPa. *Solid black contours* show the

Atlantic LLB, European, Greenland and Iberian Wave Breaking sectors as defined in Table 1. *Right panel*: 2D PDF of JLI and jet strength. PDF are mutiplied by the number of days of the dataset

Table 1 Sectors for blocking analysis

	Azores (Atlantic LLB)	Europe (EB)	Greenland (GB)	Iberian wave breaking (IWB)
	60–20W	15W–25E	65–15W	30–0W
	30–40N	50–65N	62.5–72.5N	40–50N

Fig. 2 2D PDF of JLI and jet strength composited on blocking occurring in different sector. From *lower left*, clockwise: IWB, Greenland, European blocking. *Lower right panel* shows the jet distribution when no blocking is occurring in neither of the three above-mentioned sector
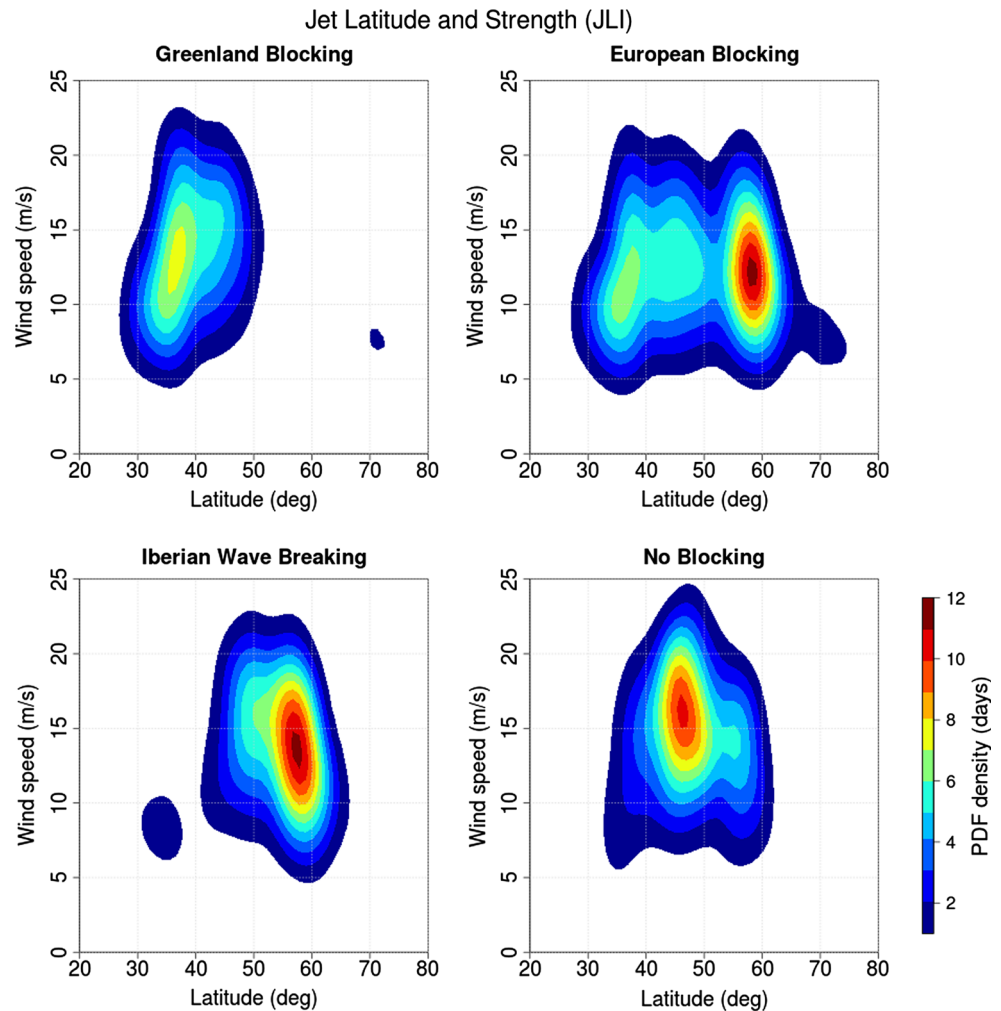
association between blocking and northward jet displacement is found for blocking events occurring over Eastern Atlantic (IWB, lower left panel)

The 2D PDF for the EB (upper right) is also associated with a northernmost occurrence of the jet, even though the jet can still be found in other locations, with a secondary preference for the equatorward position.

Excluding the days when a blocking is detected in these three reference regions (EB, GB and IWB), the JLI distribution becomes almost unimodal, as shown by lower right panel of Fig. 2. This distribution is very likely representative of the "neutral mean state" of the jet that resembles the "non-perturbed state" proposed by Woollings et al. (2010a). Moreover, when LLB is occurring the JLI PDF

(not shown) is very similar to the "no blocking" situation, confirming that these events are unable to divert the jet.

Overall, these findings are partially contrasting the results from Woollings et al. (2010a, 2011), even though they used a different blocking index. They found the same coupling between GB and southward displaced jet, and similar results between IWB region and poleward displaced jet. However, they concluded that EB is "remarkably decoupled" from the jet stream, but the results presented here show that EB is mainly associated with the poleward displacements of the jet stream. Indeed, during EB events, the probability of finding the jet in the poleward position is double with respect to the equatorward one (upper right panel of Fig. 2).

Further evidence of the major role played by EB during poleward displacements of the jet is reported in Fig. 3. Here the approach is reversed, compositing blocking events frequency on the jet latitudinal position. In left panel, the upper tail of the JLI PDF is chosen (maximum poleward displacements) and in the right panel the lower tail is selected (maximum equatorward displacements). The two tails have been defined as a function of the quartiles of the JLI PDF. The maxima are placed over Iceland and Greenland in the left panel, and over Great Britain in the right one, with the blocking frequency reaching values around the 40 %. The coupling between the northward jet displacements and the EB events is therefore evident.

These findings strengthen the idea that the displacements of the jet stream in the Atlantic basin are associated with blocking events, and more specifically, that EB is a fundamental element during the northward displacements of the jet stream. More importantly, without blocking occurrence the variability of the jet is confined around its central position (or viceversa, without jet variability no blocking is occurring).

Looking back at the climatological values of blocking frequency (left panel of Fig. 1) it is possible to notice that the distinction between the boxes labelled EB and IWB is arbitrary. The area of relative maximum, shaded in yellow, does not present any relative minimum that may suggest the presence of different preferential blocking regions. This region is spread uniformly over Western-Central Europe and Eastern Atlantic, with the maximum between Norway and the British Isles. D12 showed that blocking in this region is characterized by anticyclonic wave breaking, barotropic cross-section and similar values of duration. Since in the previous analysis we noticed that both IWB and EB sectors are associated with poleward displacements of jet, we speculate that no phenomenological difference exists between these two sectors.

In order to validate this hypothesis and to understand to what extent this blocking-jet coupling can be considered linear in space, further analyses have been performed. In the upper panel of Fig. 4, for each grid point along the red line crossing the Eastern Atlantic and Europe, the position of the jet (i.e the JLI value) is studied. For each longitude along this line (which identifies the region where anticyclonic wave breaking dominates on the equatorward side of the jet stream) the PDFs of the JLI during blocked days are constructed and plotted with colors along the y-axis. Redder colors shows preferential position of the jet stream when blocking is occurring at corresponding grid point on the red line.

The LLB over the Central and Eastern Atlantic reflects the "non-perturbed" state of the jet, where the jet lies generally around 50°N. This is more or less its average position (right panel of Fig. 1). While we move along the blocking region on the equatorward side of the jet, the jet shifts northward almost linearly (in space), reaching maximum latitudes of about 65°N in proximity of the British Isles (about 0°W). Here, blocking events split the JLI distribution in two branches, one generally lying at about 60°N and the other one at 40°N. However, the jet keeps its preferential position to the north of the block, as shown also by Fig. 2. This last feature very likely occurs because of the nature of the blocking itself, which is generally originated from an anticyclonic Rossby Wave Breaking, in which subtropical air moves north-eastward (not shown).

A different approach leading to similar conclusions is shown in the lower panel of Fig. 4. The average values of JLI during blocking days over the whole Euro-Atlantic basin is analyzed together with its associated standard deviation for every grid point. Here it is again possible to see that if blocking is detected at 40°N (i.e. LLB events), the jet is found about ten degrees to the north with very small variability. Looking poleward of 40°N, it is evident

Fig. 3 Blocking frequency for days of occurrence of the extreme quartiles of the JLI PDF. *Left panel* is upper tail of the PDF, *right panel* is the lower tail. Contours are drawn every 10 %
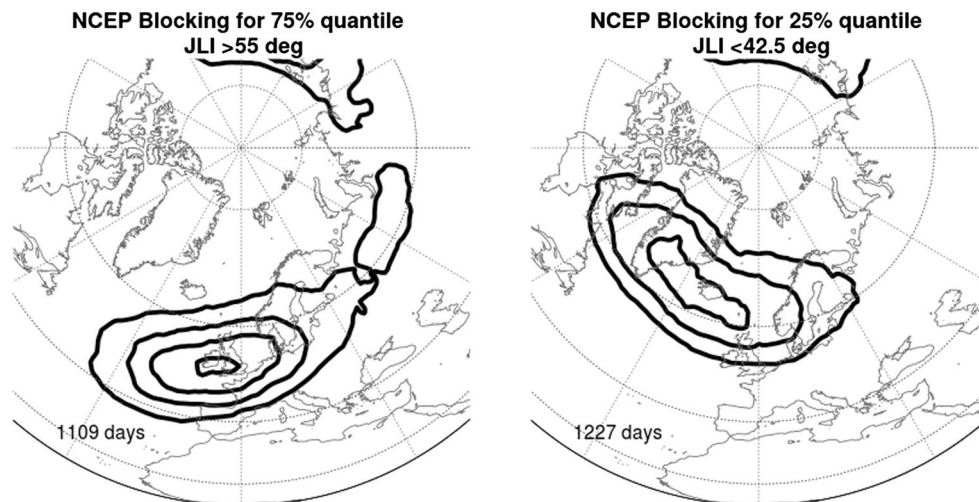

NCEP Blocking for 75% quantile
JLI >55 deg

1109 days

NCEP Blocking for 25% quantile
JLI <42.5 deg

1227 days

Fig. 4 *Upper panel*: PDFs of JLI during blocked days (*colours*) for NCEP/NCAR reanalysis computed for each grid point along the *red line*. The *red line* depicts the blocking along the equatorward side of the jet stream (see text for details). Blocking events climatology is represented by contours, drawn at 8 and 12 %. PDFs are mutiplied by the number of days of each dataset. *Lower panel*: Average JLI (*color*) and JLI standard deviation (*contours*) during blocked days for each grid point. Values are plotted only for blocking frequency exceeding 2 %
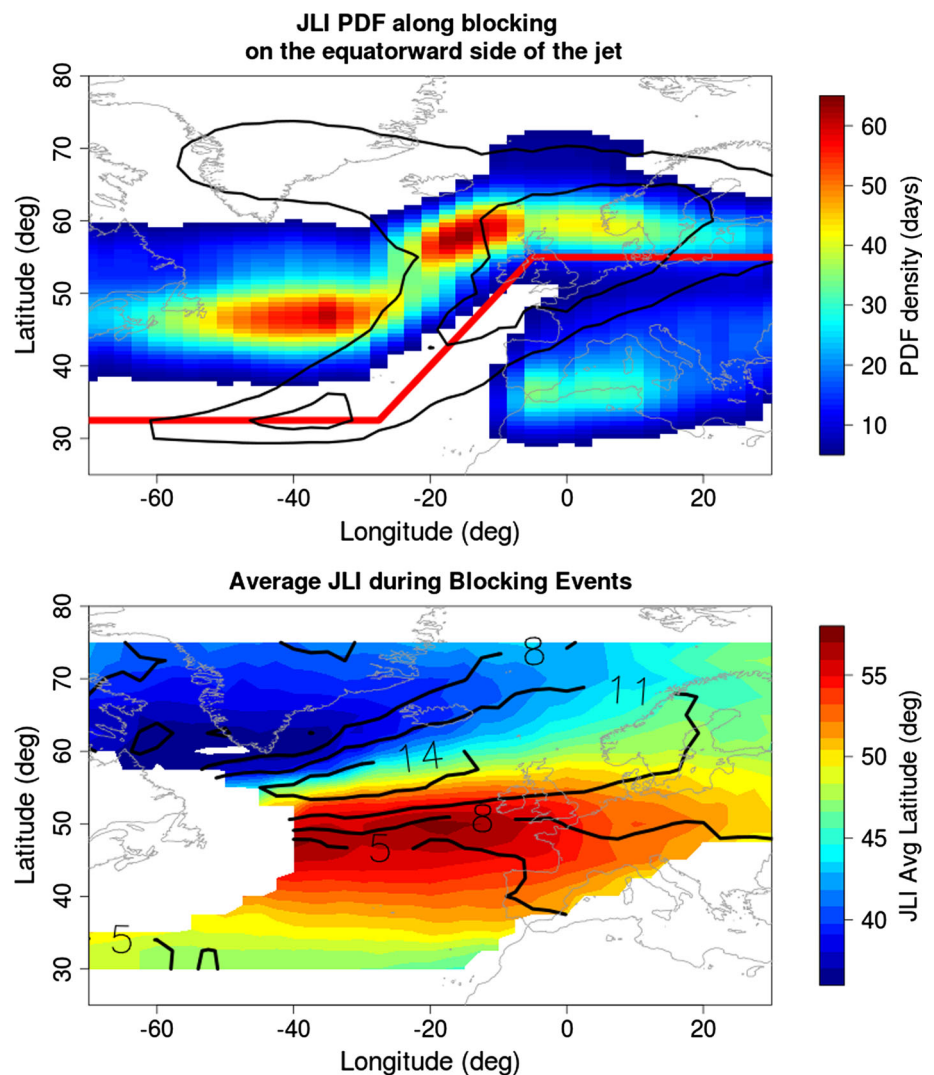
that the more to the north the blocking develops, the more to the north the jet is found. This occurs from the Azores up to the British Isles, where the standard deviation becomes very large abruptly, suggesting very high variability. On the contrary, the blue colors and small standard deviation at higher latitudes show that blocking over Greenland, Iceland and Eastern Canada favors the southward jet position.

Therefore, from our analysis it emerges as impossible to distinguish blocking events occurring over the whole European area (ranging from the Azores up to Scandinavia). This suggests that the entire blocking occurring equatorward of the eddy driven jet are associated with the northward displacement of the jet.

These findings partially conflict the idea of the four weather regimes over the Atlantic basin (3 jet positions + European blocking; Cassou et al. 2004; Woollings et al. 2010a). The "southward displaced jet/Greenland blocking regime" and the "not perturbed jet/no blocking" are evident also in our analysis. On the other hand, with the

diagnostics here adopted, it is hard to discriminate between the "poleward displaced jet" and the "European/Scandinavian blocking" regimes. We do not state that such distinction is not reliable, since it is demonstrated by several methods of analysis (i.e. EOFs and cluster analysis, e.g. Vautard 1990; Michelangeli et al. 1995; Cassou et al. 2004), but we argue that, unlike the first two regimes we analyzed, these latter have the same physical origin. Indeed, they are both consequences of the Rossby Wave Breaking on the equatorward side of the jet.

Since the jet penetration over Europe can have large variations, it is reasonable to assume that if wave breaking is occurring farther east and north, the subtropical air is able to penetrate over central Europe and the anticyclonic circulation is becoming independent from the jet, causing EB farther east that are not connected with the jet stream. This hypothesis has been validated analyzing the JLI PDF when blocking is occurring in a blocking sector further east, placed at $50°-65°N$ $15°-30°E$ (not shown). Indeed,
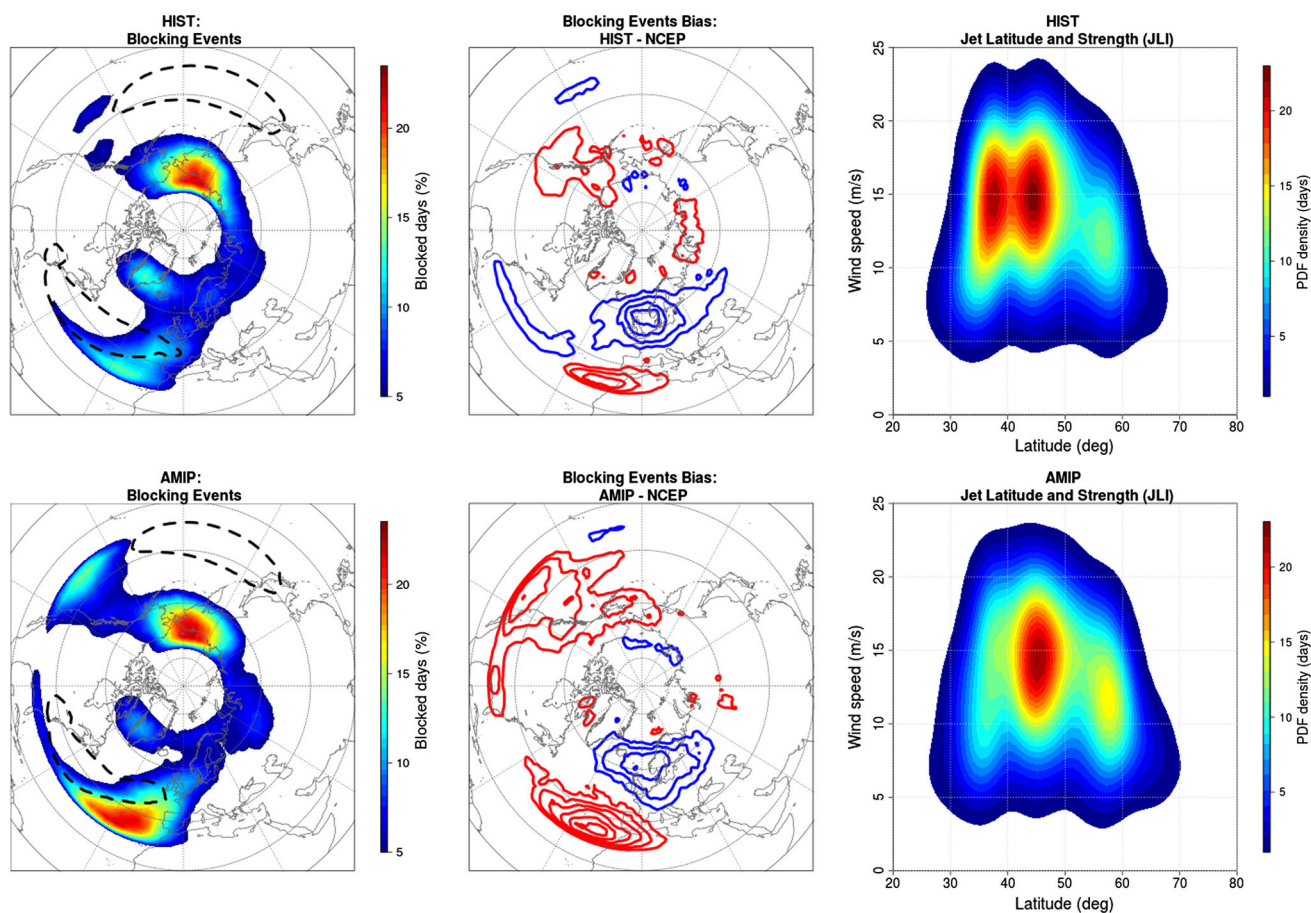
Fig. 5 *Left panel*: Same as Fig. 1 but for CMCC-CMS HIST/AMIP runs (*upper/lower panel*). *Central panels*: Difference between HIST/AMIP and NCEP-NCAR Reanalysis (*upper/lower panel*). *Blue contours* shows negative bias, *red contours* show positive bias and they are drawn every 2 %. *Right panel*: 2D PDF of JLI and jet strength for HIST and AMIP (*upper* and *lower panel*). PDF are multiplied by the number of days of the dataset

the proportion of the peaks of this PDF is the same as the climatological case.

A last consideration regards the JLI during the blocking lifecycle (not shown). We observed on average about 2 days lag between the beginning of the jet displacement and the onset of the blocking, with the former leading. However, this feature does not provide any information about any cause-effect mechanism, since it is well-known that before blocking onset (i.e. the occurrence of a wave breaking) the Z500 anomaly and its associated wave must amplify and grow. During this stage the jet is already shifting, whilst the reversal of the meridional gradient is not yet observed.

3.3 Blocking and Atlantic jet stream in the CMCC-CMS climate model

Figure 5 shows the blocking climatology for the same period for the HIST simulation (upper left panel) and the difference with respect to the NCEP/NCAR Reanalysis

(upper central panel). The simulation exhibits a large underestimation of the EB, associated with an eastward displacement of the blocking on the equatorward side of the jet (blue/red dipole over the Eastern Atlantic). Moreover, the HIST run presents a slight overestimation of the events over Greenland, whereas over the North Pacific the representation of the blocking is more accurate. However, also in this case a little eastward shift is visible, with a moderate increase of the events over the Eastern Pacific at the edge of the storm track region.

Figure 5 also shows the same diagnostics for the AMIP run (lower left and central panels), showing that with realistic SSTs, a noticeable increase in blocking frequency is obtained almost everywhere. This is especially true at low latitudes, leading to a marked overestimation of blocking over the Eastern Pacific and the Atlantic LLB area. Conversely, imposed SSTs provide also a small decrease in the bias over Europe. Finally, it is possible to see that the blocking frequency is slightly reduced over Greenland and more generally at high latitudes over the Atlantic.

In addition to this, it is possible to see that in the HIST run the climatological Atlantic eddy-driven jet stream is stronger (not shown), broader and more penetrating over Europe than in NCEP/NCAR Reanalysis and in AMIP run (dashed contour in the left panels of Fig. 5 and in Fig. 1, respectively). This last feature is very likely connected to the lowest blocking frequency reported over the Eastern Atlantic: under a climatological point of view, a reduced (increased) number of blocking events will imply a stronger (weaker) jet at the end of the storm track. This conclusion is in agreement with the findings obtained in D12 with different Reanalysis datasets.

Figure 5 also reports the 2D PDF for the JLI and the jet strength (right panels). While HIST shows an evident negative bias in the poleward displaced peak and a positive one in the equatorward displaced peak, AMIP presents a smaller bias in both peaks (compare with right panel of Fig. 1). With respect to the NCEP/NCAR Reanalysis PDF, both simulations show an equatorward displaced central peak (about $3°-4°$). However, the poleward and equatorward simulated peaks are approximatively placed at the same latitudes as in the reanalysis. Interestingly, the meridional position of the three peaks is approximately the same in both the HIST and the AMIP experiments, whereas minor changes can be observed in the jet speed. This suggests that the impact of different SSTs may change only the frequency of occupancy of the three peaks, but not their latitudinal position.

Moreover, the speed values of the central peak are also well represented by both the simulations. This apparently contrasts the previously discussed findings that showed that the climatological means are characterized by (especially for HIST) a stronger and broader low level Atlantic jet stream. This occurs because the North Atlantic is a region of marked variability, therefore the jet displacements contributes notably to the mean state. An important consequence is that the mean state itself may be not representative of the "non-perturbed" state of the jet stream.

The main blocking-related diagnostics of the model are in agreement with the NCEP/NCAR Reanalysis. This is especially true for the blocking intensities, the pattern obtained in the composites analysis and the detected region of cyclonic and wave breaking (not shown). Interestingly, both simulations show similar distribution for the blocking duration (not shown) characterized by a weak but significant underestimation (NCEP/NCAR average blocking duration 7.14 days, HIST average duration 6.89 days, AMIP average duration 7.01 days). Furthermore, in some local areas as the Labrador Sea or Iceland, the difference are significant and more marked (over the Labrador Sea NCEP/NCAR 9.15 days, AMIP and HIST 6.66 and 6.51 days respectively). The significance at 95 % level has been tested with a Wilcoxon-Mann-Whitney test.

These results suggest that blocking and Atlantic jet phenomenology are reasonably well represented by the model, even if blocking duration and frequency are both underestimated over the Euro-Atlantic area.

3.4 European blocking and the Atlantic jet displacements: the role of SSTs

After having assessed the blocking and jet representation over the Euro-Atlantic, it is interesting to analyze together the biases in the blocking frequency and in the JLI distribution of the CMCC-CMS model. As shown in Fig. 5, both simulations present significant underestimation of blocking frequency over Central Europe. This region of blocking seems to have notable importance for the jet distribution, since it is associated with the northernmost position of the jet. Therefore we investigate the model biases in the JLI to see if it is in agreement with the model biases in the blocking frequency.

To simplify our approach, we used the 1-dimensional JLI PDF as done by Woollings et al. (2010a). This technique, even though it might omit some information concerning the jet speed, is used to assess the quality of the representation of the eddy-driven jet stream and its relationship with blocking in climate simulations. Figure 6 shows the JLI distribution for NCEP/NCAR Renalysis (upper panel), HIST (central panel) and AMIP (lower panel). The blue, green, orange and dotted lines are constructed as for the 2D PDF in Fig. 2. The upper panel shows similar results to that of Fig. 2, and it is reported only for comparison.

HIST (central panel) shows the above-mentioned trimodality, with the northward peak smaller and the southward peak notably larger with respect to Reanalysis. These results are consistent with the findings previously reported: the large southern peak of the JLI PDF is associated with the intense simulated GB activity, while the less frequent modeled EB and IWB events are reflected by a smaller northernmost peak of the JLI distribution. Indeed, HIST is characterized by a lack of events over Europe particularly evident in the EB and IWB region (Fig. 5). On the poleward side of the jet, a slight overestimation of the blocking frequency is present at high latitudes.

The results shown in the bottom right panel of Fig. 5 suggest improvements for the AMIP experiment. A small bias is still present in the northernmost peak, but, overall, the PDF is now close to the one obtained from the NCEP/NCAR Reanalysis. However, we speculate that this improvement may be due to the wrong reason. In Sect. 3.2 we have shown that both EB and Iberian Wave Breaking are associated with the poleward displaced jet. Therefore, it is possible that a positive blocking bias (lower central panel in Fig. 5) present in the Eastern Atlantic (i.e. broadly over
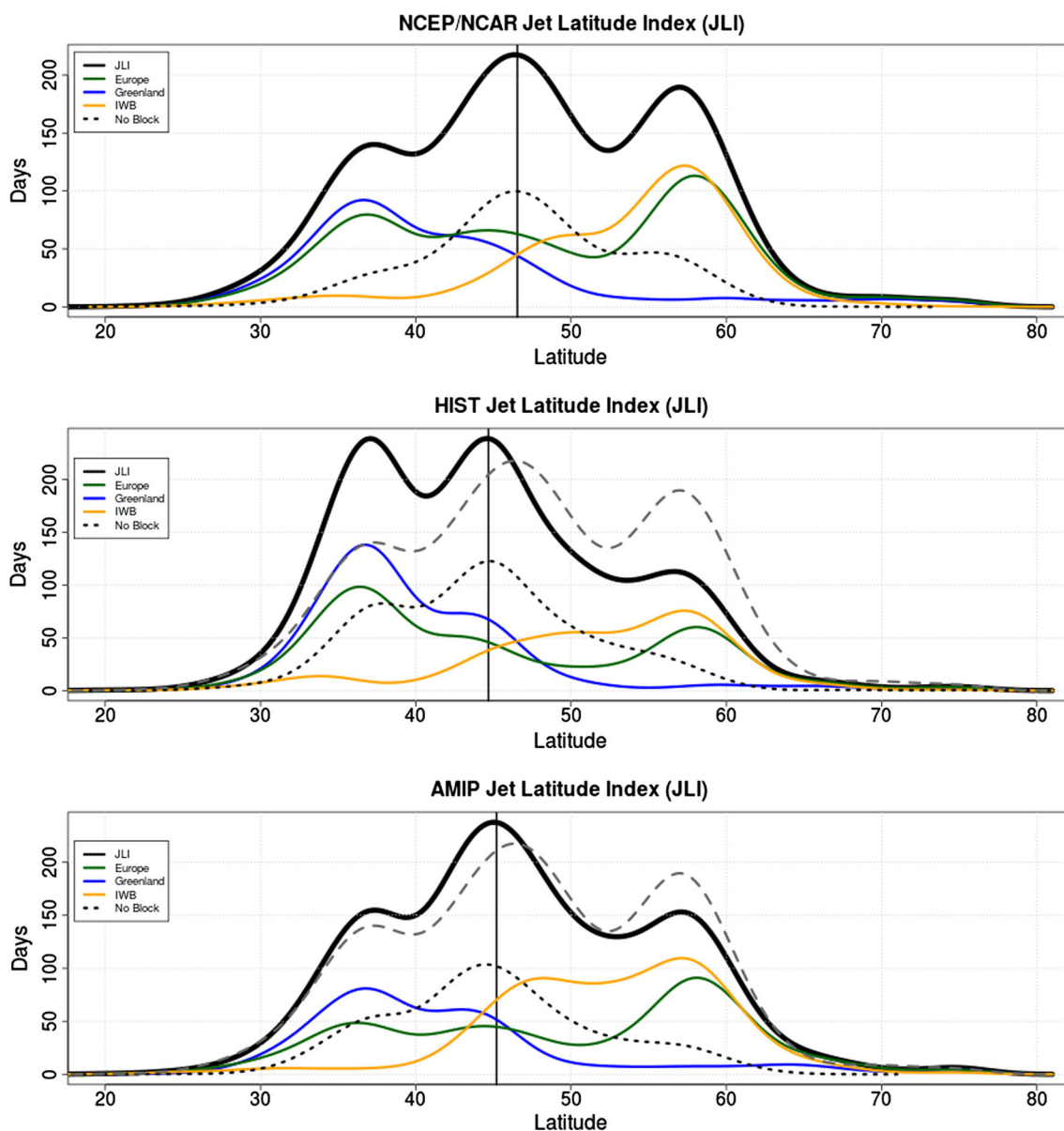
NCEP/NCAR Jet Latitude Index (JLI)

HIST Jet Latitude Index (JLI)

AMIP Jet Latitude Index (JLI)

Fig. 6 *Upper panel*: Jet latitude index PDF for NCEP/NCAR reanalysis, where *black line* represents the climatological distribution, *blue line* represents GB days, *green line* EB days and *orange line* IWB blocking days. *Dotted line* represents JLI when no blocking in the three sectors is detected. *Black vertical line* shows the latitude of the central peak. PDFs are multiplied by the number of days of each dataset. *Central and lower panel*: the same as *upper panel* but for CMCC-CMS HIST and CMCC-CMS AMIP respectively. *Dashed lines* are the JLI PDF for the NCEP/NCAR Reanalysis

the IWB sector) compensates the negative bias in the EB events. This can be seen in the lower panel of Fig. 6, where the orange line is almost doubled with respect to the HIST. In other words, the right frequency of the northward peak of the JLI PDF is obtained mainly with the overestimated numbers of IWB blocking events.

This point may have an interesting implication: a good representation of the jet variability (measured via the JLI) would not guarantee a good representation of the patterns of variability of the Euro-Atlantic sector.

Such results are in partial agreement with with the work by Scaife et al. (2011). They showed a significant improvement in blocking frequency over Europe with improved simulation of the Atlantic ocean and with imposed SSTs. They were also able to reduce the positive bias in the jet stream speed. Here, improving SSTs with imposed HadISST (AMIP run) we found an increase in the blocking over Eastern Atlantic/Western Europe (with a marked overestimation) but only a small reduction of the bias of blocking over Northern and Central Europe (Fig. 5).

On the other hand, bias in the simulated jet stream is reduced, and this is due mainly to a change in the occupation of its mode of variability.

The difference between Scaife et al. (2011) and our results may be explained by the differences in the climate models analyzed: for instance, the lower horizontal resolution of the atmospheric model here used (T63 vs N216) might be important. The possibility that the differences were arising from the different blocking indices used was also tested, but since not even the 1-dimensional Tibaldi and Molteni (1990) index was able to detect improvement in the European Blocking frequency (not shown), this hypothesis has been dropped.

Finally, we tried to investigate the reason behind the difference seen between HIST and AMIP. We thus looked at the difference between climatological SST field, shown in the left panel of Fig. 7. A cold bias over the whole Atlantic basin is evident, with a maximum of about −10 °C in the central Atlantic, south of Greenland. The right panel of Fig. 7 shows that this marked cold bias is connected with a southward displacement of the SST frontal zone. Indeed, the meridional profile of the HIST run shows a slightly stronger pole-to-equator SSTs gradient, displaced to the south by a few degrees.

The southward shift of the SSTs frontal zone is confirmed by the left panel of Fig. 7 where the HIST 10 °C isotherm, representative of the North Atlantic current path (as shown by Scaife et al. 2011), is almost 10° lat to the south with respect to the HadISST.

It is well-known that tropical SST anomalies can have an important impact on mid-latitude circulation (e.g.

Ferranti et al. 1994). However, the HIST SST bias over the tropical Atlantic is small if compared to the one observed at the mid-latitudes. We therefore preferred to focus our attention on the role played by the mid-latitude SST anomalies. Indeed, the position and the features of the mid-latitude SST front have been shown to be important for the formation of the Atlantic storm track and the eddy-driven jet stream through the creation of a strong near-surface baroclinicity area that enhances baroclinic eddy growth (Nakamura et al. 2004; Brayshaw et al. 2008; Sampe et al. 2010). More in detail, Nakamura et al (2004) showed that the climatological position of the eddy-driven jet is anchored very close to the mid-latitude SST front. Recently, Michel and Riviere (2013) noted in an aquaplanet idealized experiments that a stronger (i.e. more intense gradient) and broader frontal area is associated with a stronger eddy-driven jet stream. Furthermore, Keeley et al. (2012) showed that a large part of the bias in the North Atlantic atmospheric circulation can be associated with the cold SST bias south of Greenland (which is considerably similar to the one seen in the HIST run).

Therefore, we investigated the possibility that the differences between HIST and AMIP are caused by the bias in the simulation of the SST mid-latitude front that impacts the surface baroclinicity. Upper panels of Fig. 8 show with colors the meridional gradient of the SST field for the HIST (left) and AMIP (right). The HadISST frontal zone is sharper, but is smaller and more confined to the Western Atlantic. Conversely, the HIST SST front is wider and more extended in the Central Atlantic. The same panels show in contours the climatological eddy-driven jet stream,
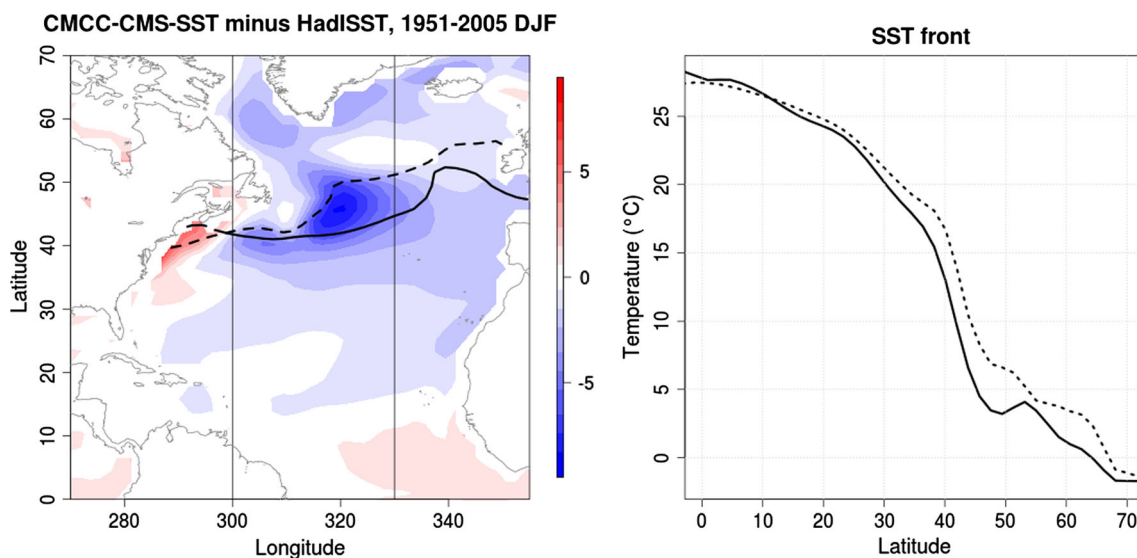

Fig. 7 *Left panel*: SST bias between the coupled CMCC-CMS HIST and the HadISST used for the AMIP run, for the DJF 1951–2005. The *solid and dashed lines* represents the position of North Atlantic current path as the 10 °C isotherm for HIST and the AMIP respectively. *Right panel*: Meridional profile of SSTs of the CMCC-CMS HIST (*solid*) and the HadISST (*dashed*), zonally averaged between 300° and 330°
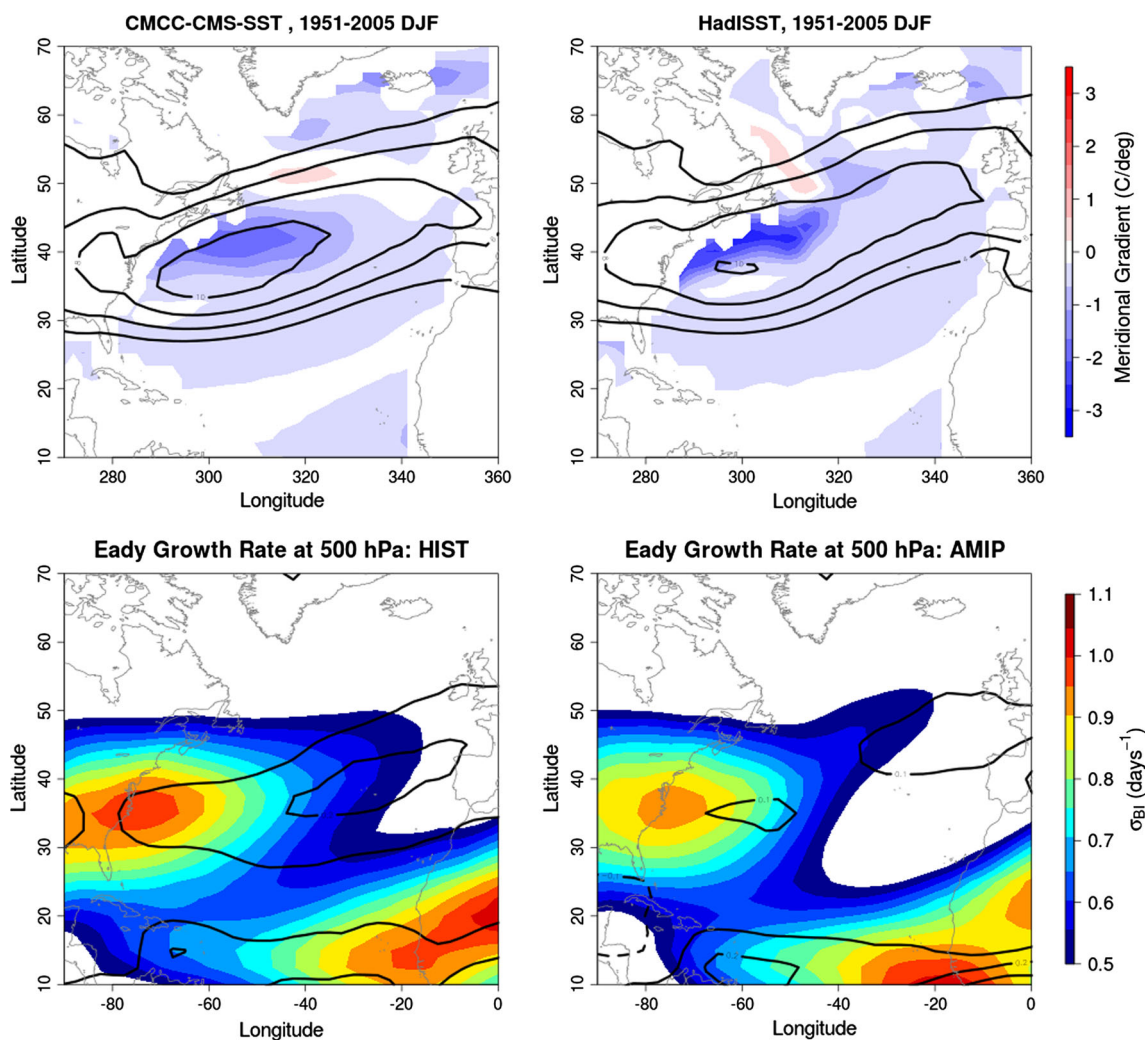
Fig. 8 *Upper panels*: SST meridional gradient (*colors*) for the coupled CMCC-CMS HIST run (*left*) and the HadISST used for the AMIP run (*right*). Atlantic eddy-driven jet as the climatological 850-hPa zonal winds is shown (*contours*). *Lower panels*: the Eady growth rate σ_{BI} at 500 hPa (*colors*) for HIST (*left*) and AMIP (*right*). Differences with respect to the NCEP/NCAR reanalysis are shown by contours

highlighting that the time averaged eddy-driven jet for the HIST is about 2 m/s stronger than the AMIP one.

All these elements suggest that a broader and equatorward displaced simulated SST front in the HIST run can be the cause of a stronger, larger, more penetrating and equatorward-displaced climatological Atlantic eddy-driven jet stream.

In order to dynamically investigate this possibility, we introduce the Eady Growth Rate (Eady 1949; Hoskins and Valdes 1990), a diagnostic providing a suitable measure of baroclinic instability. The Eady Growth Rate maximum can be defined following Vallis (2006):

$$\sigma_{BI} = 0.3068 f \left| \frac{\partial U(z)}{\partial z} \right| N^{-1} \tag{4}$$

where $U(z)$ is the vertical profile of the eastward wind component and N is the Brunt-Vaisala frequency, defined as:

$$N^2 = \frac{g}{\theta} \frac{\partial \theta}{\partial z} \tag{5}$$

The Eady Growth Rate at 500 hPa for the HIST and AMIP is reported in the lower panels of Fig. 8, together with the differences with the NCEP/NCAR Reanalysis. The HIST σ_{BI} shows higher values than the AMIP one, especially over Central and Eastern Atlantic, confirming the effect of the SST mid-latitude frontal zone on the baroclinic instability. This is in agreement with the stronger Atlantic eddy-driven jet. Qualitatively similar results are obtained computing the Eady Growth Rate maximum at different pressure levels.

Hence, our findings suggest that the stronger climatological eddy-driven jet seen in the HIST run is caused by the enhanced near-surface baroclinicity, which is in turn likely due to the larger and broader mid-latitude

SST front. Moreover, the equatorward-displaced position of the HIST run is in agreement with the few degrees displacement to the south seen in the mid-latitude SST front (right panel of Fig. 7). All these results are in agreement with previous idealized simulations performed with aquaplanet general circulation models (e.g. Sampe et al. 2010; Michel and Riviere 2013).

4 Discussion and conclusions

In this work we analyzed the relationship between the blocking activity and the eddy-driven jet stream displacements over the Euro-Atlantic sector, with a special focus on the role of European blocking. This was carried out adopting data from the NCEP/NCAR Reanalysis and from a coupled and atmosphere-only simulations of the CMCC-CMS model. The period of analysis includes the winter season (DJF) throughout 55 years (1951–2005) for the three datasets.

We showed that the majority of blocking events lying on the equatorward side of the jet, characterized by an enhanced Atlantic ridge and by an anticyclonic-wave breaking, are associated with a poleward-displaced jet. Only few EB events are clearly associated with a split flow.

Therefore we argue that the whole blocking region, lying on the equatorward side of the jet stream north of 40° N, from Azores up to Scandinavia, should be considered as a unique region when the Euro-Atlantic variability is studied. We also argue that the Atlantic LLB events over Azores can be the same manifestation of the EB, but those events are associated with wave breaking occurring too equatorward for effectively impacting the mid-latitude westerly flow. Finally, it is shown that when no blocking is occurring over the Euro-Atlantic sector, the jet stream is not perturbed and it is found in the central peak of the PDF.

Overall, these findings are partially contrasting the works of Woollings et al. (2010a), where it is concluded that European Blocking is "remarkably decoupled" from the jet stream. From the results we present here, EB appears to be mainly associated with the poleward displacement of the jet.

We can summarize by depicting a trimodal blocking-dependent Euro-Atlantic variability: when no blocking is occurring (but also during LLB events, since they cannot affect the jet stream), the Atlantic eddy driven jet is in its central "neutral" position. The equatorward jet position is linked to the occurrence Greenland blocking (and associated cyclonic wave breaking), while poleward jet position is linked to the EB (and associated anticyclonic wave breaking). EB is not confined in a small region but is originating from the breaking of the Atlantic ridge, which can occur from 30°E to 20°W (even more

to the west if LLB are also considered as a part of EB events).

Therefore EB events can have various effects on the weather pattern. Although generally EB is associated with a poleward shift of the jet, sometimes the wave breaking associated with it occurs farther East and North leading to the formation of jet-isolated strong high-pressure systems that are commonly defined as European Blocking.

This trimodal variability partially conflicts with the idea of four weather regimes usually detected over the Euro-Atlantic basin. Indeed, we showed that the "poleward displaced jet" and "European blocking" mode are substantially indistinguishable under a phenomenological point of view (i.e. vertical cross-section, associated wave-breaking orientation, duration, effects on the jet stream, etc…). Therefore we argue that, unlike the first "southward displaced jet/Greenland blocking" and the "central jet/no blocking" regimes we analyzed, the "poleward displaced jet" and the "European blocking" regimes have the same physical origin. This hypothesis is also supported by the fact that they are both associated with the Rossby Wave Breaking on the equatorward side of the Atlantic jet (Davini et al. 2012).

The results provided by the analysis of the CMCC-CMS simulations supports these conclusions. The two runs analyzed show strong bias in the simulation of the blocking on the equatorward side of the jet: they overestimate Atlantic LLB but they markedly underestimate EB.

However, different results between the two simulations are obtained for the jet stream: the fully-coupled HIST run shows a bias in the trimodal distribution of the jet stream variability, while the atmosphere-only AMIP run shows better representation of it. The main improvements interestingly regards mainly the proportion of the peaks: their position in the speed-latitude space is preserved. Especially the central peak, that represents the non-perturbed jet stream, is not influenced by the different SSTs.

Overall, there is a consistency between the biases detected in the modeled blocking frequency and the bias of the simulated Atlantic jet representation. Overestimated/ underestimated GB will be associated with increased/ decreased equatorward displaced jet, overestimated/ underestimated IWB and EB with increased/decreased poleward displaced jet. However, due to the important bias in blocking representation, further models should be considered to test the goodness of this relationship.

Importantly, the improved jet representation of the AMIP seems to be good for the wrong reasons. The strong positive bias of the blocking activity over Eastern Atlantic (i.e. over the IWB sector) seems to compensate the negative bias over Central Europe, leading to a good simulation of the jet stream variability even though the modeled blocking frequency is still underestimated. This sort of

"spurious improvement" must be considered with caution when the jet stream variability is analyzed in climate models. Hence, it is possible to state that a right representation of the jet stream variability, measured via the JLI index, could not imply a realistic simulation of the patterns of variability of the Euro-Atlantic area. This can be particularly true for Iberian Wave Breaking blocking and European Blocking, due to their association with the poleward displacements of the jet.

We analyzed the SSTs differences between HIST and AMIP, with a special attention to the characteristics and the position of the mid-latitude SST front. We noted that, in agreement with previous works, the stronger and equatorward-displaced jet found in HIST is likely due to a broader and equatorward-displaced SST frontal zone. We also checked the consistency of this idea finding higher values for the Eady Growth Rate maximum over the Central Atlantic in the HIST run.

We highlighted that in our model imposed SSTs lead to improvements in jet stream variability, but only to weak improvements in European blocking simulation in our model. This only partially confirms the work of Scaife et al. (2011), where they showed notable reduction of the bias also for blocking over Central Europe.

Finally, our results also suggest that, given the clear blocking-jet relationship, blocking can be a more accurate indicator for the Euro-Atlantic variability than the jet stream or the North Atlantic Oscillation alone. It would be therefore of striking interest to investigate these relationships in a larger group of models, as the one involved in the CMIP5 project.

References

Athanasiadis P, Wallace J, Wettstein J (2010) Patterns of wintertime jet stream variability and their relation to the storm tracks. J Atmos Sci 67(5):1361–1381

Barnes E, Hartmann D (2010) Influence of eddy-driven jet latitude on North Atlantic jet persistence and blocking frequency in CMIP3 integrations. Geophys Res Lett 37:L23,802

Barnes E, Hartmann D, Frierson D, Kidston J (2010) Effect of latitude on the persistence of eddy-driven jets. Geophys Res Lett 37: L11,804

Barnes E, Slingo J, Woollings T (2011) A methodology for the comparison of blocking climatologies across indices, models and climate scenarios. Clim Dyn:1–15

Barriopedro D, Garcia-Herrera R, Trigo R (2010) Application of blocking diagnosis methods to general circulation models. Part I: a novel detection scheme. Clim Dyn 35(7–8):1373–1391

Benedict J, Lee S, Feldstein S (2004) Synoptic view of the North Atlantic Oscillation. J Atmos Sci 66:121–144

Berrisford P, Hoskins B, Tyrlis E (2007) Blocking and Rossby wave breaking on the dynamical tropopause in the Southern Hemisphere. J Atmos Sci 64:2881–2898

Brayshaw D, Hoskins B, Blackburn M (2008) The storm-track response to idealized sst perturbations in an aquaplanet gcm. J Atmos Sci 65(9):2842–2860

Cagnazzo C, Manzini E, Giorgetta M, Foster PD, Morcrette J (2007) Impact of an improved shortwave radiation scheme in the MAECHAM5 general circulation model. Atmos Chem Phys 7:2503–2515

Cassou C, Terray L, Hurrel J, Deser C (2004) North Atlantic winter climate regimes: spatial asymmetry, stationarity with time, and oceanic forcing. J Clim 17:1055–1067

Croci-Maspoli M, Schwierz C, Davies H (2007) Atmospheric blocking: space-time links to the NAO and PNA. Clim Dyn 29:713–725

D'Andrea F, Tibaldi S, Blackburn M, Boer G, Deque M, Dix MR, Dugas B, Ferranti L, Iwasaki T, Kitoh A, Pope V, Randall D, Roeckner E, Straus D, Stern W, den Dool HV, Williamson D (1997) Northern Hemisphere atmospheric blocking as simulated by 15 atmospheric general circulation models in the period 1979–1988. Clim Dyn 14:383–407

Davini P, Cagnazzo C, Gualdi S, Navarra A (2012) Bidimensional diagnostics, variability and trends of northern hemisphere blocking. J Clim 25(19):6496–6509

Dole R, Gordon N (1983) Persistent anomalies of the extratropical northern hemisphere wintertime circulation: Geographical distribution and regional persistence characteristics. Mon Weather Rev 111(8):1567–1586

Eady E (1949) Long waves and cyclone waves. Tellus 1(3):33–52

Ferranti L, Molteni F, Palmer T (1994) Impact of localized tropical and extratropical sst anomalies in ensembles of seasonal gcm integrations. Q J R Meteorol Soc 120(520):1613–1645

Fichefet T, Morales-Maqueda M (1997) Sensitivity of a global sea ice model to treatment of ice thermodynamics and dynamics. J Geophys Res 102(12):609–646

Fogli PG, Manzini E, Vichi M, Alessandri A, Patara L, Gualdi S, Scoccimarro E, Masina S, Navarra A (2009) INGV-CMCC carbon (ICC): a carbon cycle earth system model. Report 0061, CMCC

Franzke C, Lee S, Feldstein S (2004) Is the North Atlantic Oscillation a breaking wave?. J Atmos Sci 61:145–160

Hoskins B, Valdes P (1990) On the existence of storm-tracks. J Atmos Sci 47:1854–1864

Hurrel J, Kushnir Y, Ottersen G, Visbeck M (2003) An overview of the North Atlantic Oscillation. Geophys Union Am Geophys Union 134:1–36

Kalnay E, Kanamitsu M, Kistler R, Collins W, Deaven D, Gandin L, Iredell M, Saha S, White G, Woollen J, Zhu Y, Chelliah M, Ebisuzaki W, Higgins W, Janowiak J, Mo KC, Ropelewski C, Wang J, Leetmaa A, Reynolds R, Jenne R, Joseph D (1996) The NCEP/NCAR 40-Year Reanalysis Project. Bull Am Meteorol Soc 77:437–471

Keeley S, Sutton R, Shaffrey L (2012) The impact of north atlantic sea surface temperature errors on the simulation of north atlantic european region climate. Q J R Meteorol Soc 138(668): 1774–1783

Kidston J, Vallis G (2010) Relationship between eddy-driven jet latitude and width. Geophys Res Lett 37:L21,809

Kunz T, Fraedrich K, Lunkeit F (2009) Impact of synoptic-scale wave breaking on the NAO and its connection with the stratosphere in ERA-40. J Clim 22(20):5464–5480

Kunz T, Fraedrich K, Lunkeit F (2009) Synoptic scale wave breaking and its potential to drive NAO-like circulation dipoles: a simplified GCM approach. Q J R Meteorol Soc 135:1–19

Madec G, Delecluse P, Imbard M, Levy C (1998) OPA8.1 Ocean general circulation model reference manual. Ipsl technical report, IPSL

Manzini E, Giorgetta M, Esch M, Kornblueh K, Roeckner E (2006) The influence of sea surface temperatures on the Northern winter stratosphere: ensemble simulations with the MAECHAM5 model. J Clim 19(20):3863–3881

Manzini E, Cagnazzo C, Fogli P, Bellucci A, Muller W (2012) Stratosphere-troposphere coupling at inter-decadal timescales: Implications for the north atlantic ocean. Geophys Res Lett 39:L05801

McIntyre ME, Palmer T (1983) Breaking planetary waves in the stratosphere. Nature 305:593–600

Michel C, Riviere G (2013) Sensitivity of the position and variability of the eddy-driven jet to different sst profiles in an aquaplanet general circulation model. J Atmos Sci (submitted)

Michelangeli P, Vautard R, Legras B (1995) Weather regimes: recurrence and quasi stationarity. J Atmos Sci 52(8):1237–1256

Nakamura H, Sampe T, Tanimoto Y, Shimpo A (2004) Observed associations among storm tracks, jet streams and midlatitude oceanic fronts. Geophys Monogr Ser 147:329–345

Pelly J, Hoskins B (2003) A new perspective on blocking. J Atmos Sci 60:743–755

Peters D, Waugh D (1996) Influence of barotropic shear on the poleward advection of upper-tropospheric air. J Atmos Sci 53:3013–3031

Rayner N, Parker D, Horton E, Folland C, Alexander L, Rowell D, Kent E, Kaplan A (2003) Global analyses of sea surface temperature, sea ice, and night marine air temperature since the late nineteenth century. J Geophys Res 108(D14):4407

Rex D (1950) Blocking action in the middle troposphere and its effect upon regional climate: I. An aerological study of blocking action. Int J Climatol 2:169–211

Riviere G, Orlanski I (2007) Characteristics of the Atlantic storm-track eddy activity and its relation with the North Atlantic Oscillation. J Atmos Sci 64:241–266.

Roeckner E, Brokopf R, Esch M, Giorgetta M, Hagemann S, Kornblueh L, Manzini E, Schlese U, Schulzweida U (2006) Sensitivity of simulated climate to horizontal and vertical resolution in the ECHAM5 atmosphere model. J Clim 19: 3771–3790

Sampe T, Nakamura H, Goto A, Ohfuchi W (2010) Significance of a midlatitude sst frontal zone in the formation of a storm track and an eddy-driven westerly jet. J Clim 23(7):1793–1814

Scaife A, Woollings T, Knight J, Martin G, Hinton T (2010) Atmospheric blocking and mean biases in climate models. J Clim 23:6143–6152

Scaife A, Copsey D, Gordon C, Harris C, Hinton T, Keeley S, O'Neill A, Roberts M, Williams K (2011) Improved atlantic winter blocking in a climate model. Geophys Res Lett 38(23):L23,703

Scherrer S, Croci-Maspoli M, Schwierz C, Appenzeller C (2006) Two-dimensional indices of atmospheric blocking and their statistical relationship with winter climate patterns in the Euro-Atlantic region. Int J Climatol 26:233–249

Strong C, Davis R (2008) Variability in the position and strength of winter jet stream cores related to Northern Hemisphere teleconnections. J Clim 21:584–592

Thorncroft C, Hoskins B, McIntyire M (1993) Two paradigms of baroclinic wave life-cycle behaviour. Q J R Meteorol Soc 119: 17–55

Tibaldi S, Molteni F (1990) On the operational predictability of blocking. Tellus 42:343–365

Tyrlis E, Hoskins B (2008) Aspects of a Northern Hemisphere atmospheric blocking climatology. J Atmos Sci 65:1638–1652

Valcke S (2006) OASIS3 user guide. Prism Report Series 2, CERFACS

Vallis G (2006) Atmospheric and oceanic fluid dynamics: fundamentals and large-scale circulation. Cambridge University Press, Cambridge

Vautard R (1990) Multiple weather regimes over the north atlantic analysis of precursors and successors. Mon Weather Rev 118(10):2056–2081

Woollings T, Hoskins B, Blackburn M, Berrisford P (2008) A new rossby wave breaking interpretation of the North Atlantic Oscillation. J Atmos Sci 65:609–626

Woollings T, Hannachi A, Hoskins B (2010a) Variability of the North Atlantic eddy-driven jet stream. Q J R Meteorol Soc 136: 856–868

Woollings T, Hannachi A, Hoskins B, Turner A (2010b) A regime view of the North Atlantic Oscillation and its response to anthropogenic forcing. J Clim 23:1291–1307

Woollings T, Pinto J, Santos J (2011) Dynamical evolution of North Atlantic ridges and poleward jet stream displacements. J Atmos Sci 68:954–963